Ancient midbrain inhibitory neurons control selective spatial attention

Ninad B. Kothari[1*], Wen-Kai You[1], Arunima Banerjee[1], Qingcheng Zhang[2], Shreesh P. Mysore[1,2,3,4*]

[1]*Department of Psychological and Brain Sciences, Johns Hopkins University; Baltimore MD 21218*
[2]*Undergraduate Program in Neuroscience, Johns Hopkins University*
[3]*The Solomon H. Snyder Department of Neuroscience, Johns Hopkins University School of Medicine*
[4]*Kavli Neuroscience Discovery Institute, Johns Hopkins University*
**Corresponding authors, ninadbkothari@jhu.edu, mysore@jhu.edu*

Abstract: Animal behavior at any instant is guided by information from only a subset of the plethora of stimuli in their sensory environments. The neural circuit mechanisms that select a behaviorally relevant 'target' from one location while ignoring distracting stimuli from all others remain unclear. Here, we report the discovery of an explicit neural mechanism for distracter suppression across space. In freely behaving mice engaged in a human-like task of selective spatial attention, we show that bilateral silencing of a group of parvalbumin-positive inhibitory neurons in the brainstem, PLTi, disrupts attentional target selection. This disruption occurred only when a distractor contained conflicting information, revealing that, contrary to the prevailing cortico-centric view, the brainstem PLTi is necessary for combining both top-down and bottom-up information to drive attentional target selection. Notably, unlike cortical and subcortical structures previously implicated in spatial attention, silencing of PLTi did not impair single-target visual perception, motor-plan selection or task-specific orienting movements, unveiling PLTi as a specialized brain module for competitive distracter suppression. Strikingly, PLTi also powerfully controls the accurate positioning as well as categorical precision of each animal's cognitive threshold separating the attentional target from distracters. Mechanistically, PLTi's role in attentional behavior is mediated by its sculpting of neural computations in the superior colliculus. The evolutionarily conserved PLTi may, therefore, be a dedicated brainstem engine for driving selective spatial attention in vertebrates.

One-Sentence Summary: Evolutionarily conserved inhibitory neurons in the mouse midbrain are required for ignoring distracters and selecting the next target of spatial attention.

Selective spatial attention is the remarkable ability of animals to select and preferentially process information at the most important, or "highest priority", location to guide behavior, while ignoring lower priority distractors (Carrasco 2011, Fecteau & Munoz 2006, Knudsen 2007, Mysore & Kothari 2020). This dynamic ability is essential for adaptive behavior and survival in the natural world, and is disrupted in numerous neuroatypical conditions including ADHD and schizophrenia (Luck & Gold 2008, Wender et al 2001). Research in human and non-human primates for over half a century has yielded important insights into selective spatial attention including its effects on behavior (Carrasco 2011), its effects on neural processing (Knudsen 2007, Squire et al 2013), and the brain regions involved in its operation (Basso et al 2021, Bisley & Goldberg 2010, Krauzlis et al 2013, Saalmann & Kastner 2009, Schall 2002, Squire et al 2013). However, fundamental questions about the neural basis of selective spatial attention remain open. First, the conventional view that selective spatial attention, an executive function, is controlled principally by cortical, fronto-parietal networks (Bisley & Goldberg 2010, Squire et al 2013) is a neuroethologically difficult stance to reconcile, since animals without a well-developed cortex are able to dynamically select and preferentially process behaviorally relevant subsets within the barrage of incoming information (Krauzlis et al 2018). Although some recent work has begun to contest this view (Hu & Dan 2022, Krauzlis et al 2018, Lovejoy & Krauzlis 2010), the perspective that descending signals from cortical areas predominantly drive selective spatial attention prevails (Moore & Zirnsak 2017). Second, the circuit mechanisms by which the brain *selects* the attentional target while ignoring distractors remain unknown. Indeed, how the cognitive selection boundary that separates the highest priority target from lower priority distracters is specified dynamically by brain circuitry is unclear. These neural mechanisms underlying target selection and distractor suppression are of critical import because abnormalities in selection can drive severe deficits in attention even when the neural mechanisms for the preferential processing of information remain intact (Zenon & Krauzlis 2012). Third, because the key brain regions implicated thus far in the control of selective spatial attention (Basso et al 2021, Bisley & Goldberg 2010, Krauzlis et al 2013, Squire et al 2013) are sensorimotor areas (Andersen & Cui 2009, Bisley & Goldberg 2010, Gandhi & Katnani 2011, Moore & Fallah 2001), their disruption impairs not only attention control but also a range of co-occurring functions including perception of single stimuli (Bollimunta et al 2018, Lovejoy & Krauzlis 2017, Zhou & Freedman 2019), execution of orienting movements (Bollimunta et al 2018, Dias et al 1995, Ipata et al 2006), and selection among movement plans (Cui & Andersen 2007, McPeek & Keller 2004, Wardak et al 2002). Whether, then, there exist mechanistic loci in the brain dedicated just to implementing competitive target selection and distracter suppression for selective spatial attention is unknown. Here, we address these questions in freely behaving mice engaged in a human-like task of selective spatial attention (You & Mysore 2020), and reveal the dedicated role of an evolutionarily old group of inhibitory neurons in the brainstem for distracter suppression and spatial attentional target selection.

PLTi is a conserved group of PV+ inhibitory neurons in the midbrain tegmentum that functionally inhibits the SC

Guided by three converging lines of evidence across vertebrate species, we investigated an understudied group of inhibitory neurons in the mammalian midbrain tegmentum. First, in behaving monkeys, the superior colliculus (SC; a midbrain hub that encodes multisensory and motor space topographically (Basso & May 2017)), is required for attentional target selection in the presence of distractors. Specifically, intact competitive interactions among the representations of the target and distractors across the space map in the intermediate and deep layers of SC (SCid) are critical for selective spatial attention (Krauzlis et al 2013, Lovejoy & Krauzlis 2010, McPeek

& Keller 2004). Second, although the mechanisms underlying these competitive interactions in the mammalian SCid are unknown, a potential mechanistic source (extrinsic to SC) has been identified in passive birds. Specifically, a group of parvalbumin-positive GABAergic neurons in the avian midbrain tegmentum, called Imc (nucleus isthmi pars magnocellularis), which connect bidirectionally with the OT (optic tectum, the avian homolog of SC), have been shown to orchestrate competitive stimulus interactions across the OTid (avian SCid) space map (Goddard et al 2014, Marin et al 2007, Mysore & Knudsen 2013)). Separately, these neurons have also been shown to drive competition between hemispheres in sleeping reptiles (Fenk et al 2023). Third, these inhibitory neurons, which are conserved across vertebrates (Fig. S1) (Graybiel 1978, Harvey & Worthington 1990, Jiang et al 1997, Krauzlis et al 2018), are considered to lie in the parabigemino-tegmental complex in mammals (Basso et al 2021, Graybiel 1978, Jiang et al 1997, Knudsen 2011, Krauzlis et al 2018).

To identify the relevant GABAergic neurons in the mouse parabigemino-tegmental complex (Basso et al 2021, Graybiel 1978, Jiang et al 1996, Jiang et al 1997, Knudsen 2011, Krauzlis et al 2018, Kunzle & Schnyder 1984), we immunostained for GABA in midbrain sections and found GABA+ cells distributed across this region (Fig.1A, middle; Methods). Nearly all GABA+ cells in the parabigemino-tegmental complex were also labeled for parvalbumin (PV) (Fig. 1A right – red bar plot, 95.01% ± 0.46% GABA+ cells were also PV+; Fig. 1A right – green bar plot, 94.33% ± 1.33% PV+ cells were also GABA+). Next, injection of a fluorescent tracer (Dextran; Methods) focally into the SC (Fig. 1B left, middle) showed anterogradely labeled fibers focally within the parabigemino-tegmental area (Fig. 1B-right). Conversely, injection of a cre-dependent AAV vector expressing eGFP selectively in the PV+ cells of the parabigemino-tegmental area (60 nL; AP-4.30; ML+1.75; DV-3.5; Fig. 1C, left and middle) showed anterogradely labeled fibers broadly across the intermediate and deep layers of the SC (Fig. 1C, right). Finally, selectively activating these PV+ cells in passive (head-fixed, but awake) mice using chemogenetics (Fig. 1D left; administration of chemogenetic ligand CNO vs. saline to mice expressing the excitatory chemogenetic receptor, hM3Dq, stereotactically in PV+ neurons; Methods), produced suppression of spontaneous activity in SCid (Fig. 1D middle and right; red, baseline SCid: 47.01 +/- 11.31 sp/s; 30 mins after CNO: 7.2 +/- 9.4 sp/s; 60 mins after CNO: 5.9 +/- 6.82 sp/s; blue, baseline PV+ neurons in parabigemino-tegmental complex: 5.39 +/- 14.57 sp/s; 30 mins after CNO: 35.05 +/- 15.24 sp/s; 60 mins after CNO: 34.2 +/- 12.56 sp/s Methods), revealing that they functionally inhibit SCid neurons. Thus, PV+ GABAergic neurons in the mouse parabigemino-tegmental complex receive inputs from SC, send long-range projections to SCid, and suppress SCid activity (analogously to the non-mammalian Imc neurons (Knudsen 2011, Marin et al 2007, Mysore & Knudsen 2011)). We refer to this group of PV+ GABAergic neurons in the mouse midbrain as *parabigemino-lateral tegmental inhibitory neurons* (**PLTi,** (Graybiel 1978, Jiang et al 1997)).

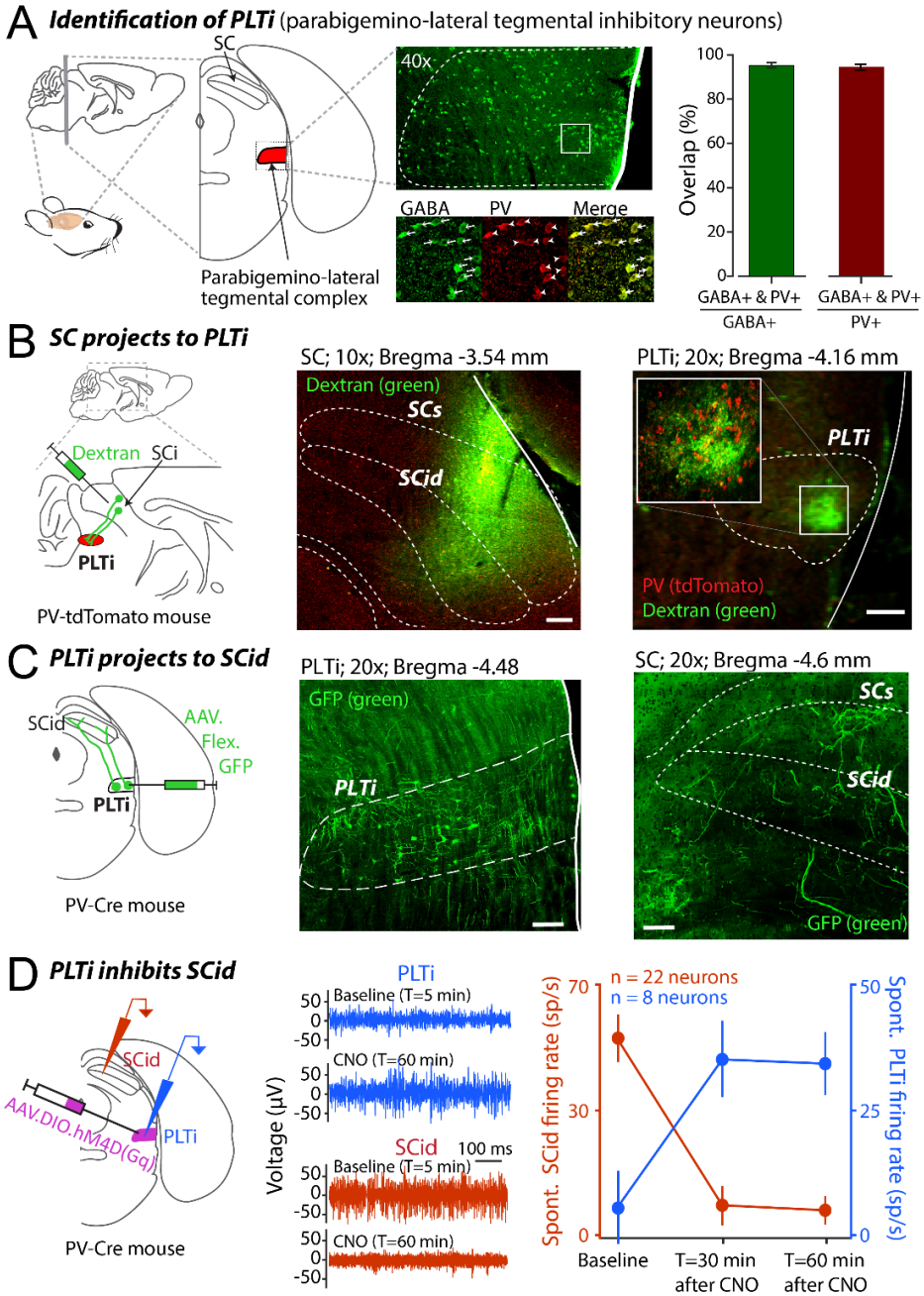

Fig. 1. PLTi is a conserved group of PV+ inhibitory neurons in the midbrain parabigemino-lateral tegmental complex that functionally inhibits the SC. (A) *Identification of PLTi (parabigemino-lateral tegmental inhibitory neurons). (Left) Anatomical location of parabigemino-lateral tegmental complex area (Methods). (Center top) Immuno-histochemical labeling of GABA+ (green) cells in this complex. Dotted line shows the outline of the complex. (Center bottom) Zoomed-in image of colocalized GABA+ (green) and PV+ (red) cells in the complex (arrows indicated cells). (Right) Summary of percentage of GABA+ cells in the complex that were also labeled for PV+ (green bar), and vice-versa (red bar; n=3 mice; see Fig. S1).* ***(B)*** *SC projects to PV+ neurons in the complex. (Left) Schematic of Dextran injection (green) in SCi (Center) injection site in the SCi (dotted white lines outline SC). (Right) Dense projection fibers (green) in the complex (dotted white lines). (Inset) Zoomed-in view of white square showing SC projection fibers (green) surrounding PV+ cells (red) in the complex.* ***(C)*** *PV+ neurons in the complex project to SCid. (Left) Schematic of location of AAV.Flex.GFP injection (green) in the complex in PV-Cre mouse and projection fibers in the SCid. (Center) Injection site in complex (dotted white lines). (Right) Projection fibers (green) in SCid (white dotted lines).* ***(D)*** *PV+ neurons in the complex functionally inhibit SCid. (Left) Schematic of location of excitatory chemogenetic injection (pink: AAV.DIO.hM3D(Gq)) in PV-Cre mouse and locations of simultaneous recordings of extracellular activity at injection site (blue) and SCid (red). (Center) Bandpass filtered extracellular activity of paired recordings from PV+ neurons in the complex (top, blue) and SCid (bottom, red). (Right) Mean activity of isolated units (n=22, two mice) in SCid measured in the baseline condition and at time points after ip injection of CNO (PLTi activated condition). All scale bars are 100 µm unless indicated. See also Fig. S1.*

PLTi controls priority-dependent target selection for visuospatial selective attention in freely behaving mice

To test the role of PLTi in the control of selective spatial attention, we trained freely behaving mice on a modified version of a touchscreen-based task of spatial selective attention we developed recently (You & Mysore 2020). (This task is modeled directly after the classic flanker task of attention in humans (Eriksen & Eriksen 1974, Fan et al 2002) (Fig. 2A, Fig. S2), and is well-known to operate on the 'priorities' of the stimuli - defined as a combination of the bottom-up (exogenous) physical salience and top-down (endogenous) behavioral relevance of each stimulus (Avital-Cohen & Tsal 2016, Fecteau & Munoz 2006)). Briefly, we trained mice to report the orientation of a central visual target - a vertical or horizontal grating, while simultaneously ignoring a peripherally located flanker (foil) - also a vertical or horizontal grating (Fig. 2A; Methods) (Avital-Cohen & Tsal 2016). Three task conditions were interleaved randomly: (a) *Target-alone condition*, in which the flanker was absent, (b) *Congruent flanker condition*, in which the target and flanker had the same orientation, and (c) *Incongruent flanker condition*, in which the target and flanker had opposite orientations (Fig. 2A). The contrast of the target was fixed while that of the flanker was varied parametrically from being lower to higher than that of the target, as a means to vary relative priority between the target and distractor (Methods, (You & Mysore 2020)). Mice were rewarded for reporting the orientation of the target with a nose-touch at the appropriate response port: horizontal (vertical) target → lower (upper) response port (Fig. 2A; counterbalanced across animals). This task design allowed the dissociation of the locus of selective spatial attention (central or peripheral azimuthal location) from the locus of behavioral report (upper or lower location).

Previous studies with the flanker task have shown that in the incongruent flanker trials, spatial attention can be captured by the flanker and drawn away from the target location, resulting in errors in performance; performance is largely unaffected in the congruent flanker trials (humans, (Eriksen & Eriksen 1974, Fan et al 2002); mice (You & Mysore 2020)). Indeed, when flanker contrast is varied, incongruent flanker trials with *low* flanker-contrasts can be defined as 'attend-towards target' trials, because in these trials, the lower priority flanker is unable to capture attention and attention is driven predominantly to the target location by the top-down spatial expectation (of potential reward). Similarly, incongruent trials with *high* flanker-contrasts can be defined as 'attend-away from target' trials, because in these trials, the higher priority flanker outcompetes the top-down expectation to the target location, and captures attention (Chung et al 2001, Fan et al 2002, Pelli et al 2004, You & Mysore 2020).

Consistent with previous studies (Eriksen & Eriksen 1974, Fan et al 2002, You & Mysore 2020), we found that mouse target selection performance in our modified flanker task was lower in incongruent flanker trials (pooled across flanker contrasts) compared to congruent flanker trials (Fig. 2B left and middle); performance was not significantly different between the congruent flanker and target alone trials (Fig. S2; (You & Mysore 2020)). Additionally, upon comparing performance in 'attend-towards target' trials (trials with the two lowest flanker contrasts) versus 'attend-away from target' trials (trials with the two highest flanker contrasts), we found higher % correct (Fig. 2B right) and higher behavioral d-prime (Fig. S2; Methods), classic signatures of selective spatial attention in primates (Lovejoy & Krauzlis 2010, Squire et al 2013)). There were no orienting differences between task conditions (Fig. S2), ruling out a purely motor related explanation for the behavioral results; other potential alternative explanations to spatial attention capture by the incongruent flanker, such as flanker and target being perceived as composites, have also been ruled out previously (You & Mysore 2020). Together, these results confirmed the

validity of the touchscreen flanker task for studying selective visuospatial attention in freely behaving mice.

With this foundation, we next tested the necessity of PLTi for selective spatial attention. We silenced the PV+ PLTi bilaterally in freely behaving mice performing the flanker task using chemogenetics (Fig. 2C left; administration of chemogenetic ligand CNO vs. saline to mice expressing the inhibitory chemogenetic receptor, hM4Di, selectively in PV+ PLTi; Methods). We found that bilateral PLTi silencing caused a dramatic drop in target selection performance in incongruent flanker trials (pooled across flanker contrasts; n= 6 PV-Cre mice; Fig. 2C middle, CNO administration, red data vs. saline administration, teal data), revealing an increase in spatial capture of attention by the incongruent flanker; performance in congruent flanker trials was unaffected (Fig. 2C middle, red vs. teal data). Bilateral PLTi silencing also caused a significant drop in the attend-towards-target performance (Fig. 2C left; and behavioral d-prime: Fig. S2). The observed deficits were not due to non-specific effects of the chemogenetic ligand, CNO: administering CNO in mice expressing a reporter but not the chemogenetic receptor produced no discernible impact on performance (Fig. S2; n=3 mice; Methods). Thus, bilateral silencing of PLTi neurons disrupted attentional target selection and caused mice to become hyperdistractible.

Considering that the flanker task operates on the priorities of stimuli (i.e., subject to top-down processing) (Avital-Cohen & Tsal 2016, Fan et al 2002), we wondered if the hyperdistractibility induced by the silencing of the brainstem PLTi was the result of PLTi neurons processing both top-down (endogenous) stimulus relevance and bottom-up (exogenous) stimulus salience (i.e., stimulus priority), or if it was the result of PLTi neurons processing just bottom-up salience (Fecteau & Munoz 2006)). We reasoned that should PLTi neurons process just stimulus salience, then silencing them in a task with a salient, but task-irrelevant, flanker should also produce hyperdistractbility. To test this, we examined the effect of bilateral PLTi silencing in a subset of mice performing a modified version of the flanker task with just one change: the oriented flanker (distractor or 'foil') was replaced by a rectangular patch of equivalent luminance (task-irrelevant distractor; n=3 PV-Cre mice; Fig. 2D left; Methods). Strikingly, we found no discernible deficits in the attend-towards performance upon PLTi silencing in the task-irrelevant flanker task (Fig. 2D right, %correct; Fig. S2, behavioral d-prime). Together with the absence of increase in RT following PLTi silencing (Fig. S2), these results demonstrated that PLTi neurons are required for priority-dependent target selection for spatial attention.

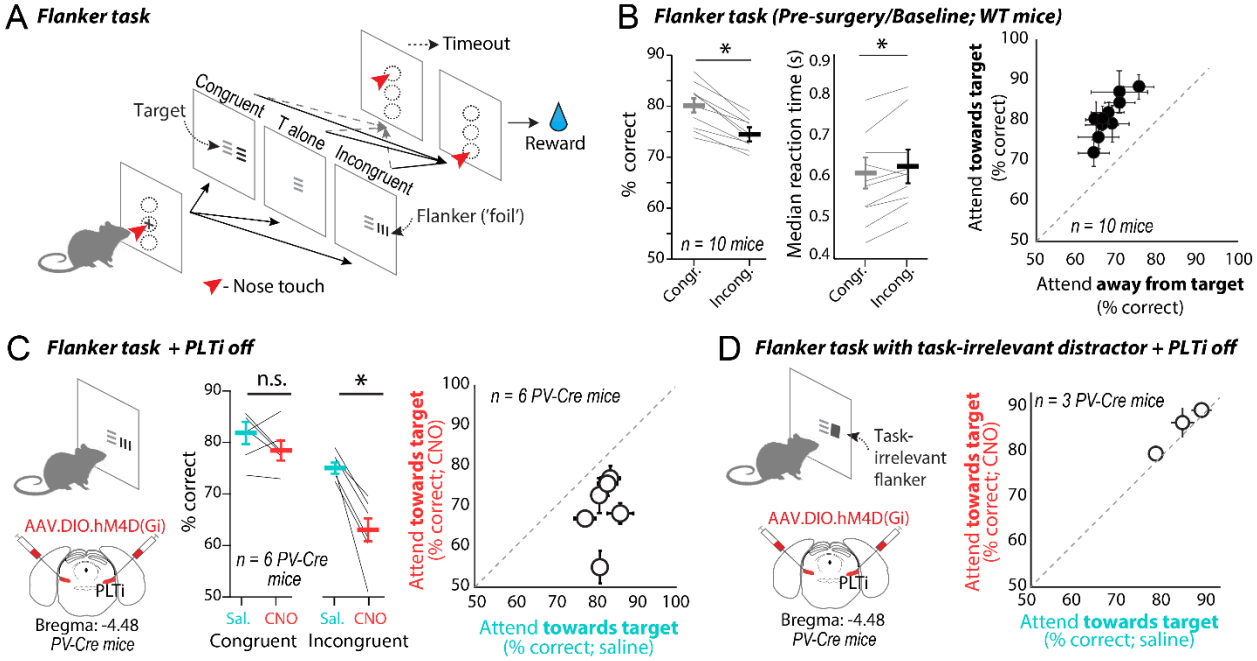

Fig. 2. PLTi controls priority-dependent target selection for visuospatial selective attention in freely behaving mice (A) *Schematic of flanker task. Vertically arranged black circles in left and right most panels show nose-poke mask used in the behavioral apparatus (also Fig. S2). Solid black arrows indicate choices leading to water reward, while dashed gray lines lead to timeouts.* ***(B)*** *Comparison of target selection performance across the congruent and incongruent task conditions pooled across contrasts; n= 10 mice. (Left) Mean percentage correct ($p=4.85*10^{-5}$, $t(9)=3.87$, paired two-tailed t-test with Holm-Bonferroni correction (HBMC) for multiple comparisons). (Center) Median RT; each line represents data from one mouse ($p=0.019$, $t(9)=2.43$, paired two-tailed t-test with HBMC). (Right) Percentage correct (mean +/- s.e.m) in the attend-toward vs. attend-away conditions (*p=0.004, t(5)=6.99, paired two-tailed t-test)*; each line - one mouse.* ***(C)*** *(Left) Abbreviated schematic of flanker task, and schematic of bilateral injection of inhibitory chemogenetic virus in PLTi of PV-Cre mouse (Methods). (Center) Comparison of target selection performance (% correct) with PLTi intact (saline -teal) and PLTi silenced (CNO-red) in congruent and incongruent task conditions, n=6 PV-Cre mice; each line - one mouse. (2-way RM-ANOVA, $p=0.00022$ for Sal vs CNO followed by HBMC between Sal and CNO for % correct: Congruent - $p=0.13$, $t(5)=1.8$; Incongruent - $p=0.002$, $t(5) = 5.6$, paired two-tailed t-tests; (see Table S1) (RT results in Fig. 3.) (Right) Percentage correct (mean +/- s.e.m) in the attend-toward condition, saline vs CNO administration ($p=0.001$, $t(5)=7.05$, paired two-tailed t-test with HBMC).* ***(D)*** *(Left) Abbreviated schematic of flanker task with task irrelevant flanker, and of bilateral chemogenetic virus injection in PLTi (Methods). (Right) Comparison of target selection performance (% correct) in attend towards condition with PLTi intact (saline) versus PLTi silenced (CNO), n=3 PV Cre mice (mean +/- s.e.m) ($p=0.66$, paired two-tailed t-test). See also Fig. S2.*

PLTi controls attentional target selection without affecting sensory perception, motor plan selection, or task-specific orienting movements

To date, the disruption of key areas implicated in selective spatial attention, such as fronto-parietal (Bisley & Goldberg 2010, Squire et al 2013) and midbrain (Basso et al 2021, Krauzlis et al 2013) areas, has been shown to also impair visual perception (perceptual sensitivity of single targets), motor plan selection (i.e., selection among orienting responses), and motor execution (i.e., trajectories and timing of orienting movements)(Basso et al 2021, Bisley & Goldberg 2010, Fecteau & Munoz 2006, Krauzlis et al 2013, Schall 2002). To what extent is the PLTi involved in any of these functions? Importantly, might potential impairments in any of these functions, rather than, specifically, in attentional target selection, explain the deficits observed in the flanker task following PLTi silencing? These are particularly germane because of the bidirectional connectivity of PLTi neurons with the SC (Fig. 1B and 1C), a major sensorimotor structure involved in all three of these functions (Basso et al 2021, Gandhi & Katnani 2011). We considered each of these functions in turn.

First, we tested if PLTi neurons influence visual perception. Results from the target alone trials of the flanker task (n = 6 PV-Cre mice; same experiments as in Fig. 2C) revealed that bilateral PLTi silencing did not significantly alter visual discrimination of single targets (Fig. S3). To test if there may be a contrast-dependent role for PLTi on visual perception, we trained a subset of mice (n=4, PV-Cre) on a single target discrimination task in which the contrast of the target (oriented grating; same as in the flanker task) was varied systematically (Fig. 3A; Methods). We found that bilateral PLTi silencing in mice performing this task as well did not alter visual discrimination performance (Fig. 3A left) or perceptual sensitivity (Fig. 3A right).

Second, we tested if PLTi neurons influence motor plan selection. In the flanker task, animals had to select between motor plans to respond at the upper port versus the lower port. Because our task design dissociated the locations of behavioral response from the locations of sensory stimulus presentation (and spatial attention, Fig. 3B left), relative response choice rates to the upper versus lower response ports was a reliable metric of motor plan selection. We found that bilateral PLTi silencing had no effect on upper versus lower choice rates in any condition of the flanker task (Fig. 3B right).

Third, we tested if PLTi neurons influence the execution of orienting movements, namely, their trajectories and their timing. We first tracked the 3-dimensional head-orienting trajectories of mice performing the flanker task using calibrated video cameras (Fig. 3C left and center, Fig. S2; n = 6 PV-Cre mice; same experiments as in Figure 2D; Methods). We found that bilateral silencing of PLTi neurons did not produce any detectable changes in movement trajectories during touchscreen interactions: either in 3D head displacement (Fig. 3C right top and Fig. S3), or in 3D head orientation (Fig. 3C right bottom and Fig. S3).

To test PLTi's role in controlling the timing of orienting movements, we analyzed mouse reaction times (RTs) in the flanker task (n = 6 PV-Cre mice; same experiments as in Fig. 2C). We found that PLTi inactivation caused *faster* (decrease in) median RTs, and did so in *all three* task conditions (T-alone, congruent and incongruent; Fig. 3D). Might an overall change in the operating point of mice along the speed-accuracy tradeoff be the reason for these faster RTs? If so, faster RTs would predict a decrease in performance (% correct) in all task conditions (Gratton et al 1988), and could potentially serve as an alternate explanation (to deficits in attentional target selection) for the lower accuracy in incongruent trials after PLTi silencing (Fig. 2D). However, we found that performance was unaffected in congruent and single target trials following bilateral PLTi

silencing (Fig. 2D and Fig. S3), ruling out a change in speed-accuracy tradeoff. How, then, might bilateral PLTi silencing cause speeding up of reaction times across task conditions? To gain insight into this question, we turned to drift diffusion modeling (DDM, (Ratcliff & Rouder 1998, Voss et al 2015)) of RT distributions from the flanker task (Methods, Fig. S3). We found that PLTi silencing caused a reduction of the threshold parameter of the DDM (threshold 'a'; Methods; Fig. S3) in each of the flanker task conditions following PLTi silencing, revealing a non-specific decrease in movement initiation threshold. Guided by this result, we hypothesized that mechanistically, such a decrease in movement thresholds would be supported by an increase in evoked firing rates of SCid neurons following PLTi silencing. This is because SCid, which receives tonic inhibition from PLTi, Fig. 1, is well-known to causally control species-relevant orienting movements across vertebrates (Allen et al 2021, Gandhi & Katnani 2011), with firing rates of SCid neurons related to thresholds for movement initiation (Herman et al 2018, Lo & Wang 2006). To test this hypothesis, we performed electrophysiological recordings in SCid of passive (head-fixed, but awake) mice (Fig. 3E left, Methods). We found that bilateral PLTi silencing caused an increase in evoked firing rates of SCid neurons to single stimuli (even) in passive mice (Fig. 3E right, Methods). Thus, the blanket increase in SCid firing rates due to PLTi silencing-induced SCid disinhibition accounted for the non-specific speeding up of reaction times across task conditions.

Together, these results demonstrated that PLTi neurons did not affect visual perception, motor plan selection, trajectories of orienting movements, or task-specific timing of orienting movements, thereby revealing a special status for PLTi, different from other areas implicated thus far in spatial attention control (Basso et al 2021, Bisley & Goldberg 2010, Krauzlis et al 2013, Schall 2002): PLTi is a dedicated module for target selection for spatial attention.

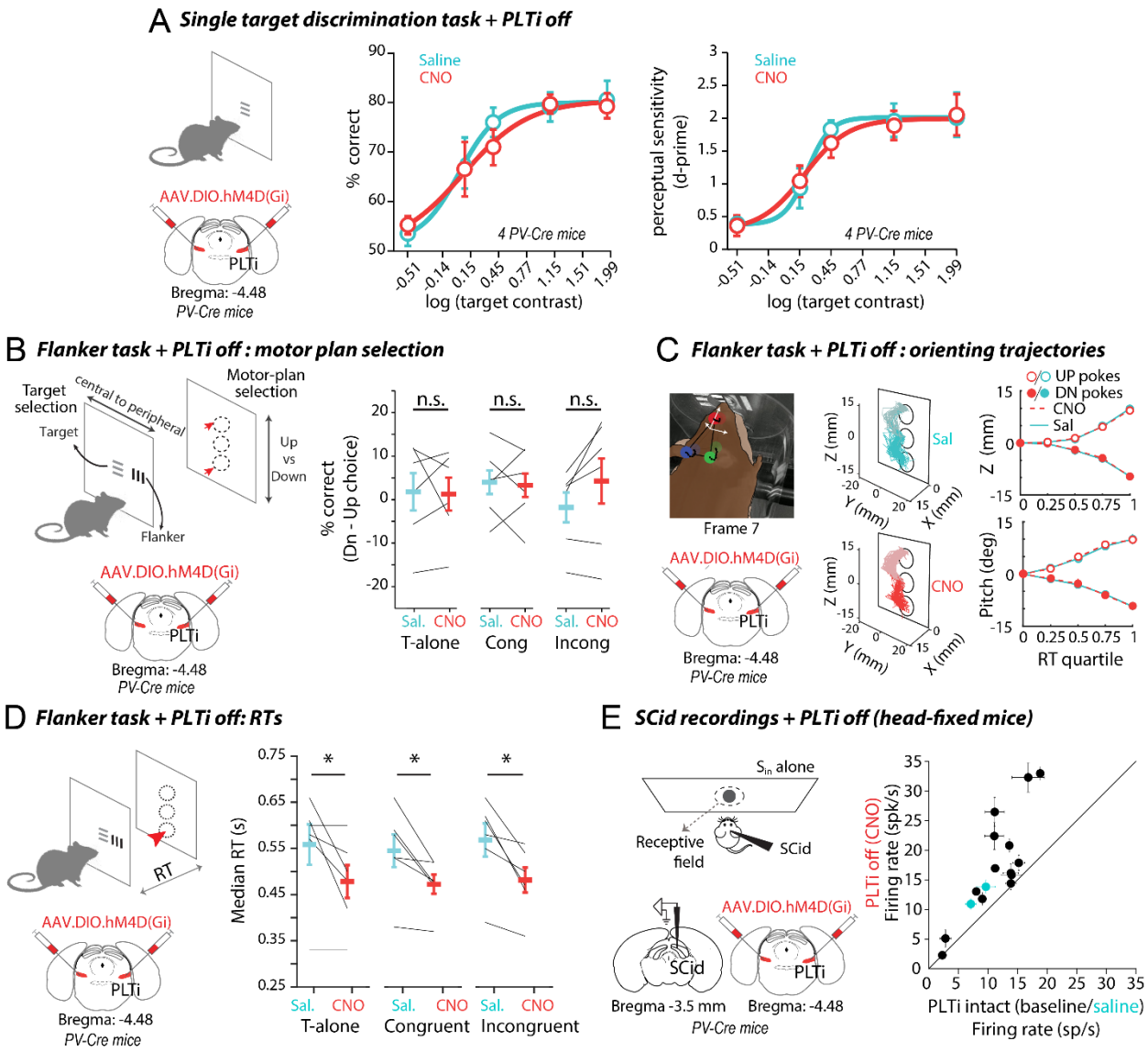

Fig. 3. PLTi controls attentional target selection without affecting sensory perception, motor plan selection, or task-specific orienting movements. (A) *(Left) Abbreviated schematic of single target discrimination task, and of bilateral chemogenetic virus injection in PLTi of PV-Cre mice (Methods). (Center and right) performance (% correct – center; p=0.81, two-way RM-anova for saline vs CNO, see Table S1) and perceptual sensitivity (right; p=0.78, two-way RM-anova, see Table S1) for the discrimination task as a function of contrast in saline (control, teal) and CNO (PLTi silenced, red) conditions, n=4 mice; mean +/- s.e.m. Solid lines - best sigmoidal fits (Methods).* ***(B)*** *(Left) Schematic of flanker task highlighting dissociation of target selection (left vs. right) and motor-plan selection (up vs. down) locations, and of bilateral chemogenetic virus injection in PLTi of PV-Cre mice (Methods). (Right) Difference in rate of selection of down vs. up choices in saline and CNO conditions. (target-only, p=0.39, t(5)=16.12, two-tailed t-test; congruent, p=0.93, t(5)=6.49, two-tailed t-test; incongruent, p=0.2, t(5)=13.92, two-tailed t-test, followed by HBMC for multiple comparisons in each case; n = 6 PV-Cre mice; same experiments as in Figure 2D. Conventions as in Fig. 2C.* ***(C)*** *(Left top) Snapshot of mouse orienting movements in a nose-poke-up choice trial, for frame #7 in trial. Red, blue and green filled circles - head-tracking labels generated by automated deep learning tool (Methods). Black dotted lines - movement trajectories across all tracked frames. White arrows - egocentric coordinate axis constructed using the three labeled markers; see also Fig. S3. (Left bottom) Schematic of virus injection in PLTi of PV-Cre mice.*

(Center) Reconstructed head movement trajectories in all saline (top, cyan) and all CNO (bottom, red) trials for an example session. Lighter colors - trials in which mouse nose-poked upper port. (Right) Head position of mouse tracked over the course of each trial; plotted as mean +/- s.e.m across trials, with each trial split into RT quartiles; (Top) Z-coordinate; (Bottom) pitch angle. Cyan-saline, red-CNO, open (closed) circles – trials with nose-poke to upper (lower) port. See Fig. S3 for X, Y coordinates and roll, yaw angles. p>0.2, for each X, Y and Z coordinates; p>0.3, for each roll, yaw and pitch angles; two-way RM-anova in each case, see Table S1. ***(D)*** *(Left) Abbreviated schematic of flanker task, and of bilateral chemogenetic virus injection in PLTi of PV-Cre mice. (Right) Median reaction times across flanker task conditions; saline (teal) vs. CNO (red); conventions as in Fig. 2C. (left, target-only, p=0.04, t(5)=2.81; middle, congruent, p=0.024, t(5)=3.11; right, incongruent, p=0.01, t(5)=3.51 – two-tailed t-tests in each case followed by HBMC).* ***(E)*** *(Left top) Schematic of experimental setup for extracellular recordings in SCid of passive, head-fixed mouse.* S_{in}*: single stimulus presented inside receptive field of SCid unit. (Left bottom) Schematic of recordings in SCid and chemogenetic virus injection in PLTi of PV-Cre mice. (Right) Mean evoked firing rates (+/- s.e.m) of SCid neurons in baseline/saline (black/teal) vs. CNO (red) conditions; n=14 units, p=0.001, t(15)=9.418, paired two-tailed t-test).*

PLTi controls the behavioral selection boundary between target and distractor, and the neural selection boundary between competing stimuli in the SC

What specific computations related to attentional target selection does PLTi regulate? Because PLTi silencing leaves single-target visual perception intact (Fig. 3A), our results thus far clearly establish that PLTi controls attentional target selection via distractor suppression. In other words, PLTi controls competitive interactions between the target and distractor. However, a critical, but unstudied aspect of such competitive interactions is how the (subjective) selection boundary that separates the highest priority target from lower priority distractors is specified neurally. The selection boundary, which dictates target selection behavior over the entire range of relative stimulus priorities, is particularly relevant to behavior in the natural world in which stimulus priorities change constantly. A mechanistic understanding of the selection boundary is, therefore, essential for elucidation of the neural basis of attentional target selection. We probed these questions next.

The defining computational attributes of the attentional selection boundary are its "position" along the axis of relative priority and its "precision" in the units of relative priority. The position of the selection boundary is the subjective value of relative priority at which target selection performance exhibits a qualitative transition in the extent to which the target is favored (Fig. 4A; dot and arrow), and the "precision" of the selection boundary is the abruptness with which this transition occurs (Fig. 4A; shading). Consequently, critical to the investigation of the position and precision of the target selection boundary is the use of a behavioral task that parameterizes attentional target selection as a function of relative priority. Our flanker task, with its parameterization of flanker priority (via parameterization of contrast) is ideally suited for this purpose (Fig. 4B, Methods). Analysis of performance in the incongruent flanker trials revealed that target selection performance (% correct) decreased as a function of flanker priority and was well-fit by a sigmoid with a well-defined transition from high to low values (Fig. 4C – example animal, Fig. S4 – summary across all animals; Methods). We quantified the position of the subjective selection boundary for each animal as the transition point of the sigmoid, i.e., the value of contrast (priority) at which accuracy was half-way between the maximum and minimum values (Fig. 4C – example animal, Fig. S4 – summary across all animals; Methods). Across animals, the position of the subjective selection boundary was 1.1 +/- 0.1 (units of log(contrast); Fig. 4D, left). We then quantified the precision of the selection boundary, i.e., abruptness of the transition, using the transition range of the sigmoid (Fig. 4C – example animal, Fig. S4 – summary across all animals;

Methods; (Mysore et al 2011)). Across animals, the transition range was narrow, and significantly smaller than that of a linear psychometric curve (Fig. 4D right; 0.37 +/- 0.07 log(contrast); Methods; Fig. 4A – black line, schematic of linear psychometric curve), demonstrating that the behavioral selection boundary in the flanker task was categorical (precise) (You & Mysore 2020). Performance in congruent flanker trials was largely unaffected by relative priority (Fig. 4C – gray points; Fig. S4 – summary across all animals). These results established that the flanker task allowed explicit quantification of the position and precision of the subjective attentional selection boundary for each animal.

Is the PLTi involved specifically in the control of the position or the precision of the attentional selection boundary? To test this, we examined the effects of bilateral chemogenetic silencing of PLTi on the relative priority-dependent psychometric selection curves (Fig 4E; Methods). We found that in the incongruent flanker trials, bilateral PLTi silencing caused both the position and the precision of the selection boundary to be impaired dramatically (Fig. 4F - example animal, same animal as in Fig. 4C; Fig. S4 – summary across all animals). The position of the subjective selection boundary was shifted leftward (Fig. 4F, example animal; Fig. 4G left and Fig. S4 – summary across animals; Methods), indicating that lower priority flankers were able to capture attention away from the target, further establishing hyperdistractibility. Additionally, the selection boundary was less precise, i.e., the response profiles became less categorical (Fig. 4F, example animal; Fig. 4G right and Fig. S4 - summary across animals; Methods). Performance in the congruent trials was unaffected by bilateral PLTi silencing (Fig. S4). These results were not due to non-specific effects of the chemogenetic ligand (CNO): administering it in mice not expressing the chemogenetic receptor produced no discernible effects in the incongruent flanker condition (Fig. S4). Thus, PLTi controls the specification of both the position and precision of the subjective attentional selection boundary in freely behaving mice.

How, mechanistically, does PLTi produce these effects? We hypothesized that PLTi may control the position and precision of the selection boundary by shaping competitive interactions and selection signals in the SCid. This hypothesis was based on the connectivity of SCid with PLTi (Fig. 1), the necessity of competitive interactions within SCid for attentional target selection in behaving monkeys (Lovejoy & Krauzlis 2010), and the demonstration in passive birds that Imc (avian PLTi) is responsible for competitive interactions within OTid (avian SCid; (Marin et al 2007, Mysore & Knudsen 2013)) and also orchestrates categorical signaling of the most salient stimulus by OTid (Mahajan & Mysore 2022, Mysore et al 2011). To test our hypothesis, we extended our recordings in passive mice (Fig. 4H; Fig. 3E) to first examine the nature of competitive interactions in mammalian SCid. We measured responses of SCid neurons to a stimulus competition protocol inspired by our flanker task (and identical to the protocol used in previous avian work (Mysore et al 2011, You & Mysore 2020); Fig. 4H-top, Methods). Briefly, we presented one stimulus, S_{in}, a dot of fixed strength (loom speed), within the spatial receptive field (RF) of the SCid neuron (typically in the binocular visual field), and a second, competing stimulus, S_{out}, of varying strength far outside the RF (typically in the peripheral visual field; Fig. 4H-top, Methods) (Asadollahi et al 2010, Mysore et al 2011). We found that responses of SCid neurons to S_{in} decreased in a sigmoidal manner with increasing salience of competitor S_{out} (Fig. 4I, example neuron). The transition point of the sigmoid (i.e., position of the neural boundary for signaling the most salient stimulus) occurred at a relative salience of zero between the competing stimuli (Fig 4I, example neuron; Fig. 4J-left, summary across neurons). In parallel, the transition range of the response profile (i.e., precision in SCid signaling of the most salient stimulus) was narrow (Fig 4I, example neuron; transition range = 0.7 deg/s; Fig. 4J right, summary across

neurons). Thus, the neural boundary separating the most salient stimulus from the others is encoded explicitly by SCid neurons in an accurate and precise (categorical) manner.

Building on this foundation, we finally examined the effect of bilateral chemogenetic silencing of PLTi on competitive interactions in the SCid of passive mice (Fig. 4K). Strikingly, we found that PLTi silencing impaired competitive interactions in SCid, specifically disrupting both the position and precision of the neural selection boundary, and in the same manner as PLTi silencing disrupts the position and precision of the behavioral selection boundary. PLTi silencing caused a leftward shift of SCid response profiles (shift in position), indicating that a weaker S_{out} was sufficient to powerfully suppress responses to S_{in} (Fig 4L, example neuron; Fig. 4M left, summary). PLTi silencing also caused the response transitions to become substantially wider (less categorical; Fig 4L- example neuron; Fig. 4M right, summary), thus decreasing the precision of the selection boundary. (Consistent with Fig. 3E, we also found an overall increase in stimulus evoked SCid firing rates during competitive interactions, Fig. S4). Considering the established necessity of intact competitive stimulus interactions in the SCid for attentional target selection (Lovejoy & Krauzlis 2010, McPeek & Keller 2004, Zenon & Krauzlis 2012), these results reveal that PLTi's shaping of competitive interactions in SCid is a major mechanistic path of action by which PLTi sets the position and precision of the attentional target selection boundary and controls target selection for spatial attention.

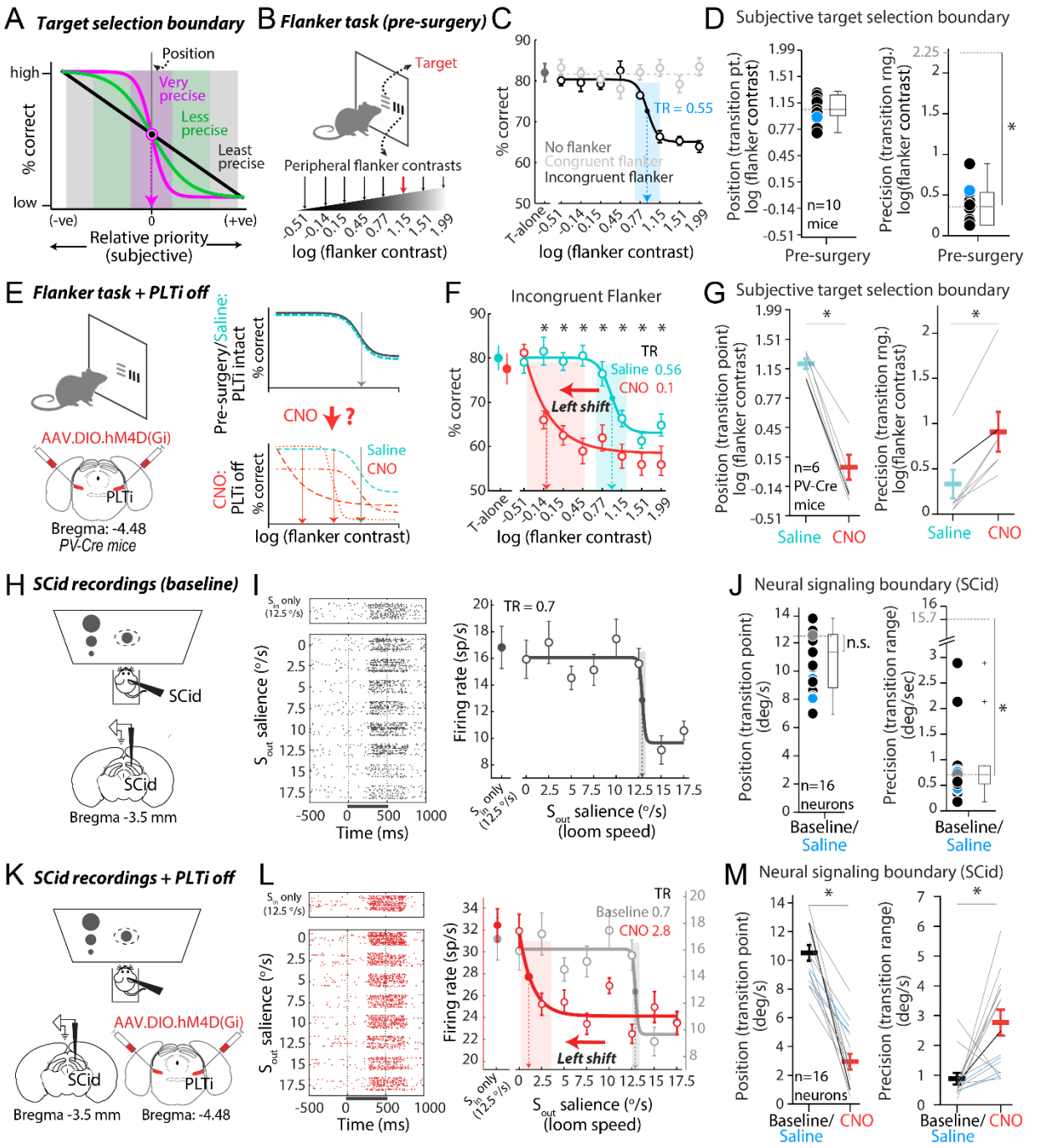

Fig. 4. PLTi controls the behavioral selection boundary between target and distractor, and sculpts the neural selection boundary in SCid (A) Illustration of position and precision of target selection boundary. Pink/green/black: three psychometric curves of target selection performance (in incongruent flanker trials) as a function of relative priority between target and distractor. Arrow: position of selection boundary (transition point – TP; Methods), at relative subjective priority =0 (by definition). Shading: precision of selection boundary (transition range – TR; Methods); pink → green → black: progressively wider TR and less precise (less categorical) selection boundary; pink – categorical psychometric profile with highly precise boundary, black – linear profile with least categorical selection boundary. **(B-D)** Position and precision of attentional target selection boundary in flanker task (incongruent flanker trials); data from same experiments as in Fig. 2B. (B) Abbreviated schematic of flanker task showing flanker contrasts (arrows) along increasing (log) scale. Red arrow: flanker and target contrasts are equal. (C) Target

selection performance (% correct) of example mouse as a function of flanker contrasts, data from incongruent (black open circles), congruent (gray open circles), and target-alone (gray solid circle) conditions; mean +/-s.e.m. Dashed light gray line: mean of congruent data. Black solid line: best sigmoidal fit to incongruent data (Methods). Blue arrow: position of selection boundary (transition point; Methods). Blue shading: precision of selection boundary, quantified by TR (transition range). (D) Summary plots showing transition points (position; left) and transition ranges (precision; right; $p=1.57*10^{-9}$, $t(9)=24.37$, paired two-tailed t-test; 2.25 = transition range of the least precise, linear selection boundary); n=10 mice. Each circle represents data from one mouse; blue circle: from example mouse in C. **(E-G)** Effect of bilateral PLTi silencing on position and precision of selection boundary in flanker task (incongruent flanker trials); data from same experiments as in Fig. 2C. (E) (Top) Abbreviated schematic of flanker task and (bottom) of bilateral injection of inhibitory chemogenetic virus in PLTi of PV-Cre mouse. (Right) Top: schematic showing baseline and saline target selection performance curves for incongruent trials as a function of flanker contrast. Bottom: hypothetical target selection performance curves after bilateral PLTi silencing, showing potential changes in the position and/or precision of the selection boundary. (F) Target selection performance (% correct) of example PV-Cre mouse as a function of flanker contrasts in incongruent trials; saline (control, cyan) vs CNO (PLTi silencing, red) conditions red vs teal, black asterisks: $p<0.05$, RM-anova and post-hoc t-tests with HBMC; each point is mean +/-s.e.m; other conventions as in C. CNO disrupts position (leftward shift) and precision (lower TR) of selection boundary. (G) Summary plots showing effect of PLTi silencing on transition points (positions; left, $p=6.04*10^{-7}$, $t(5)=4.78$, paired two-tailed t-test) and transition ranges (precision; right, $p=0.006$, $t(5)=4.55$, two-tailed t-test); n=6 PV-Cre mice; saline (control): teal; CNO (PLTi silencing): red. **(H-J)** Position and precision of neural boundary in SCid explicitly signaling the most salient stimulus. (H) (Top) Schematic of stimulus protocol for characterizing competitive interactions in SCid using two stimuli: S_{in} – receptive field stimulus and S_{out} – competing peripheral stimulus (Methods). (Bottom) Schematic showing location of extracellular recordings in SCid (Methods). (I) Responses of example SCid unit to competition protocol. (Left) Raster plot, gray bar below raster: stimulus duration. (Right) Firing rates (mean +/- s.e.m). Open circles: responses to S_{in} and S_{out}, solid line: best sigmoidal fit; solid circle: responses to S_{in} alone. Arrow: position of neural signaling boundary, close to relative salience=0, which is when S_{in} and S_{out} are equal in strength at 12.5 (deg/sec); shading: precision of neural signaling boundary. (J) Summary plots showing transition points of neural selection boundary (position; left; $p=0.125$, $t(15)=8.87$, two-tailed t-test against relative salience of 0, which corresponds to 12.5 deg/sec indicated by the gray dotted line; Methods) and transition ranges of neural signaling boundary (precision; right; $p=1.33*10^{-18}$, $t(15)=75.9$, two-tailed t-test against the TR – 15.7 deg/sec = transition range of the least precise, linear response profile; n=16 units; Methods). **(K-M)** Effect of bilateral PLTi silencing on position and precision of neural signaling boundary in SCid; panels and conventions as in H-J. (H) Schematic of flanker task, and of bilateral injection of inhibitory chemogenetic virus in PLTi of PV-Cre mouse. (L) Responses of same example SCid unit as in I to competition protocol, but with PLTi silenced (CNO, red). CNO disrupts position (leftward shift, arrows) and precision (lower TR, shading) of neural signaling boundary, wider shading (pink) implies lower precision or less categorical. (M) Summary plots of transition points (position; left, $p=1.58*10^{-7}$, $t(15)=5.95$, paired two-tailed t-test; Methods) and transition ranges (precision; right, $p=0.005$, $t(15)=3.34$, paired two-tailed t-test) of neural signaling boundary with PLTi silenced; n=16 units (lines; Methods).

Drawing inspiration from past anatomical and electrophysiological studies in birds, reptiles and amphibians (Gruberg et al 1991, Marin et al 2007, Mysore & Knudsen 2013, Sereno & Ulinski 1987), here, we discover an ancient group of PV+ inhibitory neurons in the mammalian brainstem that controls selective spatial attention. PLTi mediates priority-dependent, rather than just salience-dependent, attentional target selection: upon the silencing of PLTi neurons, it is the presence of competing misleading information (task-relevant distractor), rather than just competing salience (task-irrelevant distractor) that causes hyper-distractibility. This reveals that the brainstem PLTi integrates endogenous inputs as well as exogenous inputs to control the next target of spatial attention. PLTi does so, unlike previously identified fronto-parietal and midbrain nodes of attention (Bollimunta et al 2018, Cui & Andersen 2007, Dias et al 1995, Ipata et al 2006, Lovejoy & Krauzlis 2017, McPeek & Keller 2004, Wardak et al 2002, Zhou & Freedman 2019), without affecting visual perception, motor plan selection, or task-specific orienting, revealing it as a dedicated module for spatial attention control. This lack of PLTi's effect on orienting trajectories, when taken together with recent findings showing that freely behaving mice do not move their eyes in their head for goal directed behavior, and instead, produce orienting movements of the head to acquire targets (Meyer et al 2020), support a minimal effect of PLTi on gaze direction. Consequently, the observed impairments in attentional shifts following PLTi silencing may involve covert, rather than overt attentional shifts.

The (computational) roles of PLTi neurons in these attentional shifts are sophisticated. PLTi neurons control the degree to which attentional target selection is categorical (or step-like) as a function of relative stimulus priority. In the natural world replete with sensory ambiguity and response variability, such categorical psychometric response profiles boost reliability in selecting the highest priority target (Gollisch & Meister 2010, Mysore & Kothari 2020) - an ethologically adaptive feature. PLTi also controls the position of the selection boundary, i.e., the point of subjective equality of the priorities of the target and (task-relevant) distractor. Notably, the observed consistent shift of this boundary disfavoring the target and affording undue competitive advantage to the distractor parallels the attentional phenotype in neurodivergent conditions (including ADHD and schizophrenia; (Luck & Gold 2008, Wender et al 2001)). To date, no other circuit mechanism for the explicit control of the attributes of the attentional target selection boundary has been reported (Basso et al 2021, Bisley & Goldberg 2010, Krauzlis et al 2013, Saalmann & Kastner 2009, Schall 2002, Squire et al 2013). (We note that these attributes of the selection boundary are conceptually distinct from the frequently studied "criterion" and "perceptual sensitivity" (Luo & Maunsell 2015): while the former require parameterized investigation of attentional selection across a range of relative-priority values, the latter characterize discrimination performance at each value of relative priority, and can vary with it). Finally, our results that the effects of mispositioning and loss of precision of the behavioral selection boundary following PLTi silencing are observed also for neural signaling boundaries measured in the SCid, even in passive animals, not only reveal a mechanistic path of action for PLTi to exert its effects on attentional behavior, but also reveal the hitherto unknown mechanism underlying competitive interactions across the space map of mammalian SC (Sooksawate et al 2011).

PLTi's necessity for the executive function of selective spatial attention, despite its evolutionarily antecedence and its early station in the neural processing hierarchy (Graybiel 1978, Jiang et al 1997, Mahajan & Mysore 2018, Wang et al 2004), is striking, and promotes re-examination of traditional notions about an exclusively fronto-parietal neural basis of selective spatial attention. Moreover, PLTi's dedicated role for attentional target selection over other related sensorimotor functions supports a structured, computationally driven organization of brain

systems for selective spatial attention (Knudsen 2007, Mahajan & Mysore 2022, Mysore & Kothari 2020), in departure from recent suggestions of extraordinarily distributed neural substrates for cognitive functions (Steinmetz et al 2019, Urai et al 2022). Similar specific circuit mechanisms in the forebrain network that also influence the attentional selection boundary, and the functional logic by which midbrain and forebrain circuits of attention work together to drive behavior (Shipp 2004), remain to be understood.

Acknowledgments: We thank Sarah Correas, Samrawit Getachew, Isabel Rios Pulgar, Sarah Saccal, Marvin Lee, Huiyao Chen, Elisa Herrera, Spencer Loggia, and Ronald Salazar for help with behavioral training of the mice, and Spencer Loggia for help with the cameras. We thank Dr. Eric Garr for sharing protocols for CNO use. We thank James Garmon for engineering support. We are grateful to Dr. Howard Egeth, Dr. James Knierim and Dr. Kishore Kuchibhotla for helpful feedback on the manuscript.

Funding: This work was supported by NIH F32EY032776 (NBK), NIH R34NS111653 (SPM), NSF 2047298 (CAREER award, SPM) and start-up funds from the Johns Hopkins University (SPM).

Author contributions: SPM and NBK conceived the project and designed the experiments; NBK performed and supervised behavioral experiments and data analyses; NBK and QZ performed the electrophysiological experiments and analyses; WKY, AB and NBK performed anatomical experiments and analyses; SPM and NBK wrote the paper.

Competing interests: The authors declare that they have no competing interests.

Data and materials availability: Code, data and materials used in the analysis will be made available upon reasonable request to the corresponding author.

REFERENCES

Allen KM, Lawlor J, Salles A, Moss CF. 2021. Orienting our view of the superior colliculus: specializations and general functions. *Curr Opin Neurobiol* 71: 119-26

Andersen RA, Cui H. 2009. Intention, action planning, and decision making in parietal-frontal circuits. *Neuron* 63: 568-83

Asadollahi A, Mysore SP, Knudsen EI. 2010. Stimulus-driven competition in a cholinergic midbrain nucleus. *Nat Neurosci* 13: 889-95

Avital-Cohen R, Tsal Y. 2016. Top-Down Processes Override Bottom-Up Interference in the Flanker Task. *Psychol Sci* 27: 651-8

Basso MA, Bickford ME, Cang J. 2021. Unraveling circuits of visual perception and cognition through the superior colliculus. *Neuron* 109: 918-37

Basso MA, May PJ. 2017. Circuits for Action and Cognition: A View from the Superior Colliculus. *Annu Rev Vis Sci* 3: 197-226

Bisley JW, Goldberg ME. 2010. Attention, intention, and priority in the parietal lobe. *Annu Rev Neurosci* 33: 1-21

Bollimunta A, Bogadhi AR, Krauzlis RJ. 2018. Comparing frontal eye field and superior colliculus contributions to covert spatial attention. *Nat Commun* 9: 3553

Carrasco M. 2011. Visual attention: The past 25 years. *Vision research* 51: 1484-525

Chung ST, Levi DM, Legge GE. 2001. Spatial-frequency and contrast properties of crowding. *Vision Res* 41: 1833-50

Cui H, Andersen RA. 2007. Posterior parietal cortex encodes autonomously selected motor plans. *Neuron* 56: 552-9

Dias EC, Kiesau M, Segraves MA. 1995. Acute activation and inactivation of macaque frontal eye field with GABA-related drugs. *J Neurophysiol* 74: 2744-8

Eriksen BA, Eriksen CW. 1974. Effects of noise letters upon the identification of a target letter in a nonsearch task. *Perception & Psychophysics* 16: 143-49

Fan J, McCandliss BD, Sommer T, Raz A, Posner MI. 2002. Testing the efficiency and independence of attentional networks. *J Cogn Neurosci* 14: 340-7

Fecteau JH, Munoz DP. 2006. Salience, relevance, and firing: a priority map for target selection. *Trends Cogn Sci* 10: 382-90

Fenk LA, Riquelme JL, Laurent G. 2023. Interhemispheric competition during sleep. *Nature* 616: 312-18

Gandhi NJ, Katnani HA. 2011. Motor functions of the superior colliculus. *Annu Rev Neurosci* 34: 205-31

Goddard CA, Mysore SP, Bryant AS, Huguenard JR, Knudsen EI. 2014. Spatially Reciprocal Inhibition of Inhibition within a Stimulus Selection Network in the Avian Midbrain. *PLoS One* 9: e85865

Gollisch T, Meister M. 2010. Eye smarter than scientists believed: neural computations in circuits of the retina. *Neuron* 65: 150-64

Gratton G, Coles MG, Sirevaag EJ, Eriksen CW, Donchin E. 1988. Pre- and poststimulus activation of response channels: a psychophysiological analysis. *J Exp Psychol Hum Percept Perform* 14: 331-44

Graybiel AM. 1978. A satellite system of the superior colliculus: the parabigeminal nucleus and its projections to the superficial collicular layers. *Brain Research* 145: 365-74

Gruberg ER, Wallace MT, Caine HS, Mote MI. 1991. Behavioral and physiological consequences of unilateral ablation of the nucleus isthmi in the leopard frog. *Brain Behav Evol* 37: 92-103

Harvey AR, Worthington DR. 1990. The projection from different visual cortical areas to the rat superior colliculus. *The Journal of Comparative Neurology* 298: 281-92
Herman JP, Katz LN, Krauzlis RJ. 2018. Midbrain activity can explain perceptual decisions during an attention task. *Nat Neurosci* 21: 1651-55
Hu F, Dan Y. 2022. An inferior-superior colliculus circuit controls auditory cue-directed visual spatial attention. *Neuron* 110: 109-19 e3
Ipata AE, Gee AL, Goldberg ME, Bisley JW. 2006. Activity in the lateral intraparietal area predicts the goal and latency of saccades in a free-viewing visual search task. *J Neurosci* 26: 3656-61
Jiang ZD, King AJ, Moore DR. 1996. Topographic organization of projection from the parabigeminal nucleus to the superior colliculus in the ferret revealed with fluorescent latex microspheres. *Brain Research* 743: 217-32
Jiang ZD, Moore DR, King AJ. 1997. Sources of subcortical projections to the superior colliculus in the ferret. *Brain Res* 755: 279-92
Knudsen EI. 2007. Fundamental components of attention. *Annu Rev Neurosci* 30: 57-78
Knudsen EI. 2011. Control from below: the role of a midbrain network in spatial attention. *Eur J Neurosci* 33: 1961-72
Krauzlis RJ, Bogadhi AR, Herman JP, Bollimunta A. 2018. Selective attention without a neocortex. *Cortex* 102: 161-75
Krauzlis RJ, Lovejoy LP, Zenon A. 2013. Superior colliculus and visual spatial attention. *Annu Rev Neurosci* 36: 165-82
Kunzle H, Schnyder H. 1984. The isthmus-tegmentum complex in the turtle and rat: a comparative analysis of its interconnections with the optic tectum. *Exp Brain Res* 56: 509-22
Lo CC, Wang XJ. 2006. Cortico-basal ganglia circuit mechanism for a decision threshold in reaction time tasks. *Nat Neurosci* 9: 956-63
Lovejoy LP, Krauzlis RJ. 2010. Inactivation of primate superior colliculus impairs covert selection of signals for perceptual judgments. *Nat Neurosci* 13: 261-6
Lovejoy LP, Krauzlis RJ. 2017. Changes in perceptual sensitivity related to spatial cues depends on subcortical activity. *Proc Natl Acad Sci U S A* 114: 6122-26
Luck SJ, Gold JM. 2008. The construct of attention in schizophrenia. *Biol Psychiatry* 64: 34-9
Luo TZ, Maunsell JH. 2015. Neuronal Modulations in Visual Cortex Are Associated with Only One of Multiple Components of Attention. *Neuron* 86: 1182-8
Mahajan NR, Mysore SP. 2018. Combinatorial Neural Inhibition for Stimulus Selection across Space. *Cell Rep* 25: 1158-70 e9
Mahajan NR, Mysore SP. 2022. Donut-like organization of inhibition underlies categorical neural responses in the midbrain. *Nat Commun* 13: 1680
Marin G, Salas C, Sentis E, Rojas X, Letelier JC, Mpodozis J. 2007. A cholinergic gating mechanism controlled by competitive interactions in the optic tectum of the pigeon. *J Neurosci* 27: 8112-21
McPeek RM, Keller EL. 2004. Deficits in saccade target selection after inactivation of superior colliculus. *Nat Neurosci* 7: 757-63
Meyer AF, O'Keefe J, Poort J. 2020. Two Distinct Types of Eye-Head Coupling in Freely Moving Mice. *Curr Biol* 30: 2116-30 e6
Moore T, Fallah M. 2001. Control of eye movements and spatial attention. *Proc Natl Acad Sci U S A* 98: 1273-6
Moore T, Zirnsak M. 2017. Neural Mechanisms of Selective Visual Attention. *Annu Rev Psychol* 68: 47-72

Mysore SP, Asadollahi A, Knudsen EI. 2011. Signaling of the strongest stimulus in the owl optic tectum. *J Neurosci* 31: 5186-96
Mysore SP, Knudsen EI. 2011. The role of a midbrain network in competitive stimulus selection. *Curr Opin Neurobiol* 21: 653-60
Mysore SP, Knudsen EI. 2013. A shared inhibitory circuit for both exogenous and endogenous control of stimulus selection. *Nat Neurosci* 16: 473-8
Mysore SP, Kothari NB. 2020. Mechanisms of competitive selection: A canonical neural circuit framework. *Elife* 9
Pelli DG, Palomares M, Majaj NJ. 2004. Crowding is unlike ordinary masking: distinguishing feature integration from detection. *J Vis* 4: 1136-69
Ratcliff R, Rouder JN. 1998. Modeling Response Times for Two-Choice Decisions. 9: 347-56
Saalmann YB, Kastner S. 2009. Gain control in the visual thalamus during perception and cognition. *Curr Opin Neurobiol* 19: 408-14
Schall JD. 2002. The neural selection and control of saccades by the frontal eye field. *Philos Trans R Soc Lond B Biol Sci* 357: 1073-82
Sereno MI, Ulinski PS. 1987. Caudal topographic nucleus isthmi and the rostral nontopographic nucleus isthmi in the turtle, Pseudemys scripta. *J Comp Neurol* 261: 319-46
Shipp S. 2004. The brain circuitry of attention. *Trends Cogn Sci* 8: 223-30
Sooksawate T, Isa K, Behan M, Yanagawa Y, Isa T. 2011. Organization of GABAergic inhibition in the motor output layer of the superior colliculus. *Eur J Neurosci* 33: 421-32
Squire RF, Noudoost B, Schafer RJ, Moore T. 2013. Prefrontal contributions to visual selective attention. *Annu Rev Neurosci* 36: 451-66
Steinmetz NA, Zatka-Haas P, Carandini M, Harris KD. 2019. Distributed coding of choice, action and engagement across the mouse brain. *Nature* 576: 266-73
Urai AE, Doiron B, Leifer AM, Churchland AK. 2022. Large-scale neural recordings call for new insights to link brain and behavior. *Nat Neurosci* 25: 11-19
Voss A, Voss J, Lerche V. 2015. Assessing cognitive processes with diffusion model analyses: a tutorial based on fast-dm-30. *Front Psychol* 6: 336
Wang Y, Major DE, Karten HJ. 2004. Morphology and connections of nucleus isthmi pars magnocellularis in chicks (Gallus gallus). *J Comp Neurol* 469: 275-97
Wardak C, Olivier E, Duhamel JR. 2002. Saccadic target selection deficits after lateral intraparietal area inactivation in monkeys. *J Neurosci* 22: 9877-84
Wender PH, Wolf LE, Wasserstein J. 2001. Adults with ADHD. An overview. *Ann N Y Acad Sci* 931: 1-16
You WK, Mysore SP. 2020. Endogenous and exogenous control of visuospatial selective attention in freely behaving mice. *Nat Commun* 11: 1986
Zenon A, Krauzlis RJ. 2012. Attention deficits without cortical neuronal deficits. *Nature* 489: 434-7
Zhou Y, Freedman DJ. 2019. Posterior parietal cortex plays a causal role in perceptual and categorical decisions. *Science* 365: 180-85